The Journal of Neuroscience, July 1991, 11(7): 2226–2240

Halothane Inhibits Two Components of Calcium Current in Clonal (GH_3) Pituitary Cells

James Herrington,[1,2] Richard C. Stern,[1] Alex S. Evers,[1] and Christopher J. Lingle[1]

[1]Department of Anesthesiology, Washington University School of Medicine, St. Louis, Missouri 63110, and [2]Department of Biological Sciences, The Florida State University, Tallahassee, Florida 32306

The effect of halothane on isolated calcium (Ca^{2+}) current of clonal (GH_3) pituitary cells was investigated using standard whole-cell clamp techniques at room temperature. Halothane (0.1–5.0 mM) reversibly reduced both the low-threshold, transient [low-voltage-activated (LVA)] component and the high-threshold [high-voltage-activated (HVA)] component of Ca^{2+} current. Halothane had little effect on the voltage dependence of activation or inactivation of either component of Ca^{2+} current. Inhibition of the peak high-threshold Ca^{2+} current was half-maximal at about 0.8 mM halothane, with maximal inhibition (100%) occurring with 5 mM halothane. When measured at the end of a 190-msec command step, half-maximal reduction of high-threshold current occurred at less than 0.5 mM halothane. The low-threshold transient current was less sensitive to halothane, with half-maximal inhibition of peak transient current activated at −30 mV occurring at approximately 1.3 mM.

The effect of halothane on the HVA current was apparently not mediated by changes in intracellular Ca^{2+} concentration. The ability of halothane to inhibit Ca^{2+} current was unaffected by either the inclusion of the rapid Ca^{2+} buffer 1,2-bis(2-aminophenoxy)ethane *N,N,N′,N′*-tetraacetic acid (BAPTA) in the recording pipette or exposure of the cell to 10 mM caffeine.

To assess the selectivity of the effect of halothane, the actions of halothane on two components of voltage-activated potassium (K^+) current observed in the absence of extracellular Ca^{2+} and on voltage-dependent sodium (Na^+) current were also examined. Halothane had no effect on the voltage-dependent, inactivating K^+ current of GH_3 cells at concentrations up to 1.2 mM. In contrast, the non-inactivating K^+ current, though less sensitive to halothane than either Ca^{2+} current, was reduced by about 40% by 1.2 mM halothane at +20 mV. Peak Na^+ current was also blocked by halothane, but 50% block required around 2.6 mM halothane with little effect at 1.6 mM. Reduction of Na^+ current was associated with a substantial negative shift in the steady-state inactivation curve. Although the results indicate that a number of voltage-dependent ionic currents are sensitive to halothane, both components of Ca^{2+} current exhibit a greater sensitivity to halothane than any of three other voltage-dependent currents in GH_3 cells.

These results show that GH_3 cell Ca^{2+} currents are selectively inhibited by clinically appropriate concentrations of halothane and that the reduction of Ca^{2+} current can account for the inhibition by halothane of TRH- or KCl-induced prolactin secretion in GH_3 cells.

The production of anesthesia by volatile anesthetics is thought to be a consequence of depression of CNS excitability or an inhibition of synaptic transmission (e.g., Larrabee and Posternak, 1954; Richards and Smaje, 1976; Richards, 1983; Takenoshita and Takahashi, 1987; Kullmann et al., 1989; Miu and Puil, 1989; Pearce et al., 1989). The underlying mechanism of volatile anesthetic action presumably involves alteration of one or more membrane conductances, though as yet there has been little success in attempting to correlate anesthetic action with effects on any specific membrane current. For example, halothane has been shown to reduce Na^+ current both in neuronal (Bean et al., 1981; Haydon and Urban, 1983) and in a number of non-neuronal preparations (heart muscle: Ikemoto et al., 1986; skeletal muscle: Ruppersberg and Rudel, 1988). However, the reduction of Na^+ current by halothane occurs at clinically unreasonable concentrations. At lower concentrations, halothane hyperpolarizes spinal motor neurons, hippocampal pyramidal cells (Nicoll and Madison, 1982), and some snail neurons (Franks and Lieb, 1988) by activating a K^+ conductance. Whether activation of a K^+ current participates in any of the clinical effects of halothane remains an open question.

Recent evidence suggests that halothane can also inhibit voltage-dependent Ca^{2+} current at clinically reasonable concentrations both in neurons (Krnjević and Puil, 1988) and in heart muscle (Terrar and Victory, 1988). Because of their central importance in both neuronal excitability and synaptic transmission, Ca^{2+} channels would be of particular interest as potential targets for volatile anesthetic action. In neurons, either of two types of high-threshold Ca^{2+} currents may be important in synaptic transmission (Rane et al., 1987; Hirning et al., 1988; Holz et al., 1988; Bean, 1989a), while low-threshold Ca^{2+} currents may play a role in determining patterns of action potential firing (Llinas and Yarom, 1981; Llinas, 1988; Suzuki and Rogawski, 1989). Several recent reports support the view that both low- and high-threshold forms of Ca^{2+} channels are inhibited by volatile anesthetics (Eskinder et al., 1990; Herrington and Lingle, 1990; Takenoshita and Steinbach, 1990).

As one approach to understanding the mechanisms of volatile anesthetic action, we have been using the GH_3 clonal pituitary

Received Nov. 20, 1990; revised Feb. 15, 1991; accepted Feb. 25, 1991.

We thank Sandra Leal for technical assistance and E. McCleskey, J. Nerbonne, and J. Steinbach for comments on the manuscript. This work was supported by NIH Grant RO1 DK37109 to C.J.L. and RO1 GM37846 to A.S.E. R.C.S. was supported by a Burroughs Wellcome/Foundation for Anesthesia Education and Research fellowship. A.S.E. is an Established Investigator of the American Heart Association.

Correspondence should be addressed to Dr. Chris Lingle, Department of Anesthesiology, Washington University School of Medicine, Box 8054, 660 South Euclid Avenue, St. Louis, MO 63110.

cell line as a model system in which the effects of halothane on a secretory process can be investigated at a number of levels. In the preceeding article (Stern et al., 1991), halothane was shown to reduce secretion of prolactin and attendant elevations of $[Ca^{2+}]_i$ when these effects were associated with influx of Ca^{2+}. Here, we examine directly the effects of halothane on GH_3 cell Ca^{2+} current to determine whether these effects of halothane can be accounted for by changes in Ca^{2+} current. GH_3 cells are known to exhibit two distinct components of Ca^{2+} current (Armstrong and Matteson, 1985; Matteson and Armstrong, 1986), a transient current activated by depolarization to relatively negative command potentials [low-voltage activated (LVA)] and a relatively noninactivating current activated by depolarizing steps to more positive threshold potentials [high-voltage activated (HVA)]. Both currents can be reliably voltage clamped and well separated. Furthermore, effects of agents on Ca^{2+} current can be compared to effects on a number of other voltage-dependent currents (Dubinsky and Oxford, 1984; Matteson and Armstrong, 1984).

The results show that the reduction of Ca^{2+} current by halothane probably accounts for the inhibition of stimulus–secretion coupling produced by halothane in GH_3 cells. Furthermore, the results of this and the preceding article (Stern et al., 1991) show that, of a number of membrane-associated processes, only Ca^{2+} currents are altered by clinically appropriate concentrations of halothane. The concentration dependence of the blockade of Ca^{2+} current by halothane in GH_3 cells is, at the least, consistent with the possibility that some clinical effects of halothane may reflect direct blockade of Ca^{2+} current.

Materials and Methods

Cell culture. The GH_3 cell line was obtained from the American Tissue Type Collection (Rockville, MD). Cells were grown as described in the accompanying article (Stern et al., 1991). Cells for electrophysiological experiments were grown on poly-L-lysine coated pieces of glass coverslips and used between 1 and 19 d after plating. Cells from passages 21–28 were used in the experiments described in this article.

Electrophysiological recording. Recordings were made using standard dialyzed-cell voltage-clamp techniques (Hamill et al., 1981). Electrodes were pulled from aluminosilicate glass (A-M Systems, Everett, WA), coated with Sylgard (Dow Corning, Midland, MI), and fire polished. Pipette resistances were 1.5–4 MΩ. Voltage commands and digitization of membrane currents were done using the PCLAMP software package (Axon Instruments, Foster City, CA) running on an IBM AT-class computer. Membrane currents were recorded using an Axopatch 1B patch-clamp amplifier (Axon Instruments). For measurement of Ca^{2+} currents, only recordings in which the series resistance was 4–15 MΩ was used. Because maximal Ca^{2+} currents were usually much less than 500 pA, series resistance compensation was usually not employed. For salines used for recording Na^+ and K^+ currents, the series resistance was typically less than 5 MΩ. All experiments were done at room temperature (20–23°C).

Solution exchange procedures. Pieces of glass coverslips were transferred to a rectangular chamber of 7 mm width and a total volume of less than 0.5 ml. Four separate perfusion lines entered the chamber at one end, while solution was removed from the other end using suction. The perfusion rate was 2.5 ml/min. Switching between solutions was accomplished by manually controlled valves. Test solutions were maintained in all-glass syringes closed with weighted glass syringe plungers. The glass syringe plungers were allowed to fall by gravity. Differences in residual pressure following positioning of the plungers within the syringes clearly result in a net positive pressure on the backs of the syringes that may differ between test solutions. The effect of such pressure differences was minimal in the bath-exchange system used here. In control experiments, switching between perfusion lines with each line containing control saline resulted in no effect on GH_3 cell Ca^{2+} currents. In contrast, with either localized puffer applications of control saline or switching between control salines using a local microperfusion system, we encountered substantial changes in Ca^{2+} current amplitude.

Data analysis. Voltage-activated currents recorded during experiments were stored digitally without leakage subtraction. Currents generated by hyperpolarizing commands applied before and after test protocols were stored separately for subsequent off-line digital subtraction of leakage and capacitive currents. Leakage currents were subtracted for all current traces except those shown in Figures 1, 3, and 10. Fitting of currents and of extracted data was accomplished using a nonlinear least-squares procedure based on the Levenberg–Marquardt routine [RMSSQ subroutine of the IMSL statistical library (Bellaire, TX)] for minimization of residuals. Values reported in the text for sets of estimates represent means and standard deviations. Fitted values are reported with either a 90% or a 95% confidence limit.

Determination of anesthetic concentration. Halothane-containing salines were prepared by diluting a saturated solution of the anesthetic in saline (17 mM, 20°C) to the desired final concentrations. Volatile anesthetic concentrations in saline from samples taken from the recording chamber were routinely measured by gas chromatography (Stern et al., 1989). Unless otherwise indicated, all concentrations stated in this article are measured values obtained from samples of the experimental solutions flowing into the bath.

Anesthetic potency is most frequently reported in terms of partial pressure in gas. Halothane concentrations in gas of 1, 2, and 3 vol% correspond to concentrations of halothane in saline of 0.5, 1, and 1.5 mM at 23°C and 0.25, 0.5, and 0.75 mM at 37°C. This reflects the greater solubility of halothane in saline at low temperatures. A parallel twofold increase in the potency of halothane (when measured as anesthetic concentrations in the gas phase) occurs over the same temperature range (Cherkin and Catchpool, 1964; Regan and Eger, 1967). Thus, equal concentrations of halothane in saline should be approximately equipotent at 23°C and 37°C. From the present experiments, the clinically relevant range of halothane in saline was defined as ≈0.3–3 times the EC_{50} of halothane in the rat. The EC_{50} of halothane in the rat at 37°C is 1.24 vol% (Evers et al., 1986), which corresponds to a concentration of halothane of 0.31 mM in saline. Thus, we consider the concentration range of halothane in saline that would correspond to the anesthesia-producing effects of halothane to be ≈0.1–0.93 mM.

Commercially available halothane contains thymol, a preservative. To test the possibility that the effects described here might reflect an action of thymol on Ca^{2+} current, thymol-free halothane solutions were prepared. This was accomplished by volatilizing halothane in air using a temperature-compensated vaporizer. Thymol is not volatile and remains behind in the vaporizer. The vaporized, thymol-free halothane was then bubbled through saline, and the concentration of halothane in the resulting salines was determined by gas chromatography as described above. Thymol-free solutions of halothane produced identical effects on Ca^{2+} current as those with thymol.

Recording solutions. Salines used for the isolation of Ca^{2+} current were (in mM)—Internal: 140 tetramethylammonium hydroxide (TMA-OH), 10 EGTA, 40 HEPES, 2 $MgCl_2$, 4 Na_2ATP, 0.5 cAMP, and 0.05 GTP; pH 7.1–7.3 with methanesulfonic acid (CH_4O_3S); External: 100 Tris-OH, 50 tetraethylammonium hydroxide (TEA-OH), 10 glucose, and 10 $CaCl_2$, pH 7.4 with CH_4O_3S. In some experiments, 10 mM Cs_4-1,2-bis(2-aminophenoxy)ethane *N,N,N',N'*-tetraacetic acid (Cs_4-BAPTA) was substituted for 10 mM EGTA in the internal saline. Cells were generally maintained in a sodium-based physiological saline until seal formation, at which time the bath was switched to the Tris/TEA saline. Salines used for potassium current experiments were (in mM)—Internal: 120 K-aspartate, 30 KOH, 10 EGTA, 40 HEPES, 2 $MgCl_2$, 4 Na_2ATP, and 0.05 GTP; pH 7.1–7.3 with *N*-methyl-D-glucamine (NMG); External: 140 Na-isethionate, 5.4 K-gluconate, 10 glucose, 10 Na-HEPES, 4 $MgCl_2$, and 0.00025–0.0004 tetrodotoxin (TTX); pH 7.4 with CH_4O_3S. Sodium current was isolated with the following salines (in mM)—Internal: 140 CsF, 14 NaF, 1 EGTA, 10 HEPES, and 2 $MgCl_2$; pH 7.15 with NMG; External: 145 Na-isethionate, 10 Na-HEPES, 10 glucose, and 4 $MgCl_2$; pH 7.4 with CH_4O_3S. The osmolarity was 300–315 mOsm for extracellular solutions and 285–300 mOsm for intracellular solutions.

In a number of experiments, LVA current was examined under conditions in which HVA current had completely run down (Armstrong and Eckert, 1987). In such experiments, the run-down process was facilitated by the use of the following fluoride-based intracellular saline (in mM): 140 TMA-OH, 10 EGTA, 40 HEPES, and 2 $MgCl_2$; titrated to pH 7.15 with HF.

Chemicals. Halothane was obtained from Ayerst Laboratories (New York, NY). BAPTA was obtained from Molecular Probes (Eugene, OR). All other chemicals were from Sigma (St. Louis, MO) or Aldrich Chemicals (Milwaukee, WI).

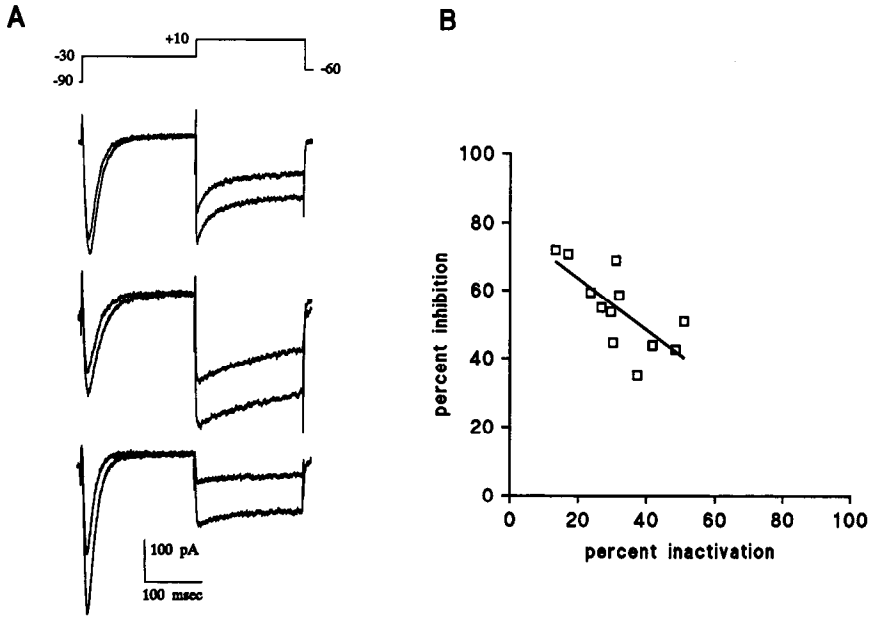

Figure 1. Halothane reduces both LVA and HVA Ca^{2+} current in rat GH_3 clonal pituitary cells. In *A*, a standard voltage-step protocol used for examination of Ca^{2+} current activated at low threshold potentials and at higher threshold potentials is illustrated at the *top*. From a holding potential of −90 mV, the cell potential was stepped to −30 mV for 200 msec and then stepped to +10 mV for 190 msec before returning to −60 mV. Representative currents evoked in three different cells are shown *below* the voltage protocol. In each case, following the step to −30 mV, a transient inward current (LVA) is observed that inactivates virtually completely within the 200-msec command step. Following the step to +10 mV, a more slowly inactivating inward current (HVA) is observed. The *middle two sets* of current traces show the effect of 0.5 mM halothane, while the *bottom set* of traces shows the effect of 1 mM halothane. Halothane produces a small reduction in current activated at −30 mV and a more pronounced reduction in peak current activated at +10 mV. Note that the fractional block by halothane of HVA current is more pronounced at the end of the command step to +10 mV in each case. Traces were uncorrected for leakage and capacity transient currents. Series resistances (R_s) for each cell were 11.0, 9.0, and 13.5 MΩ, from top to bottom. Cell capacitances (C_m) were 31.5, 15.4, and 35.8 pF. In *B*, the fractional blockade of peak HVA current by 1 mM halothane for 12 cells is plotted as a function of the percent of the total HVA current exhibiting inactivation over the 190-msec step to +10 mV. The *line* over the points is a fitted line to indicate the trend of the points and not based on any particular model of the properties of peak and sustained HVA current. The correlation coefficient for the line was −0.72. The effect of halothane on peak HVA current is weaker when HVA current is composed of a larger fraction of inactivating current.

Results

The results address three distinct topics. First, the qualitative effects of halothane on two components of Ca^{2+} current in GH_3 cells are demonstrated. Second, the relative lack of effect of halothane on both voltage-dependent Na^+ and K^+ current is shown. Third, an examination of some potential mechanisms by which halothane might reduce each component of Ca^{2+} current is provided.

Halothane reduces both high- and low-threshold Ca^{2+} current in GH_3 cells

The presence of two distinct components of Ca^{2+} current in clonal pituitary cells, distinguishable on the basis of kinetic properties, voltage dependence, inactivation, and pharmacology, is well established (Armstrong and Matteson, 1985; Matteson and Armstrong, 1986; Cohen and McCarthy, 1987). One current is activated by membrane potentials positive to about −40 mV and appears to exhibit complete inactivation over most or all of its activation range. This current appears similar to the LVA or T-current described in vertebrate neurons (Carbone and Lux, 1984, 1987; Bossu et al., 1985; Yoshii et al., 1988; reviewed by Bean, 1989a). A second current in GH_3 cells is activated by more positive command potentials and exhibits little or only slow inactivation. This latter current is reminiscent of HVA or L-current observed in neurons (Fox et al., 1987; reviewed by Bean, 1989a). No evidence has been presented to support the possibility that clonal pituitary cells may exhibit a third type of Ca^{2+} current analogous to the inactivating, high-threshold N-current observed in some neurons (Fox et al., 1987; Kostyuk et al., 1988; reviewed by Bean, 1989a). Here rapidly inactivating currents activated at lower threshold potentials will be termed LVA Ca^{2+} currents, while relatively non-inactivating currents activated at more positive threshold potentials will be termed HVA Ca^{2+} currents.

The basic procedure used here for separation of the two components of Ca^{2+} current is shown in Figure 1*A*. Currents from three cells are shown in order to illustrate the variability in properties of HVA current. LVA Ca^{2+} current was activated by stepping to −30 mV from a holding potential of −90 mV. Virtually all current activated at −30 mV inactivates, indicative that no detectable HVA current has been activated (e.g., see Figs. 1, 8–10). Thus, measurement of peak inward current activated by steps to −30 mV largely reflects the exclusive activation of LVA current. This is consistent with the observations of Matteson and Armstrong (1986), who showed that little high-threshold current was activated even at −20 mV.

To allow examination of HVA current, following the activation and inactivation of LVA current at −30 mV the cell membrane potential was stepped to +10 mV. Such steps revealed considerable variability in the extent and rates of inactivation of HVA current among cells. As shown in Figure 1, HVA current could be either largely noninactivating or slowly inactivating. The inactivating current does not reflect the con-

tribution of LVA current, because as shown below (see Fig. 10), LVA current is completely inactivated by the prepulse to −30 mV. Assuming that the HVA current reflects a single type of Ca^{2+} current, the variability in the inactivation process may reflect differences in the amount of Ca^{2+}-dependent inactivation of Ca^{2+} current (Kalman et al., 1988), perhaps reflecting variations among cells in Ca^{2+} buffering. However, the amount of inactivation was not dependent on the series resistance of the recording pipette, eliminating one simple explanation for differences in cellular Ca^{2+} buffering. It is also unlikely that the inactivation reflects an unidentified outward current. The ionic conditions of these experiments (low Cl^-; extracellular saline: 50 mM TEA and 100 mM Tris; intracellular saline: 140 mM TMA) provide no reasonable candidates to support outward current of any type.

The ability of halothane to reduce both LVA and HVA Ca^{2+} current is also illustrated in Figure 1*A*. For the three cells shown, Ca^{2+} currents both in control saline and in the presence of halothane are displayed. The records indicate that HVA Ca^{2+} current is more sensitive to halothane than LVA Ca^{2+} current. One complication, which is particularly apparent with HVA currents that show a substantial inactivating component, is that current activated in the presence of halothane has a shape parallel to that in the absence of halothane. Halothane appears to remove a relatively noninactivating portion of HVA current. Thus, the fractional blockade at the end of the command step is greater than at the beginning of the command step. This effect is summarized in Figure 1*B*, in which the fractional blockade of peak HVA current is shown to be inversely correlated with the amount of inactivating current (see also Fig. 4*B*). Such an effect would be consistent with the presence of two distinct HVA currents, a relatively non-inactivating or slowly inactivating current more sensitive to halothane and an inactivating current more resistant to halothane. However, alternative explanations involving changes in the equilibrium among different states of a single type of HVA channel are also possible. Here, no further attempt will be made to evaluate the significance of inactivation of HVA current in the GH_3 cells in our cultures.

Stability of halothane blocking action

The stability and reproducibility of the action of halothane was examined in experiments in which the same concentration of halothane was applied repeatedly to a voltage-clamped cell while Ca^{2+} current was elicited at 15-sec intervals with the standard protocol used in Figure 1. As illustrated in Figure 2*A*, the reduction of HVA Ca^{2+} current produced by 1.0 mM halothane was relatively constant for three different applications applied over an 8-min period. Similarly, as shown in Figure 2*B* for a different cell, the blocking effect of halothane was identical irrespective of the duration of halothane action up to about 4 min of application. There is no indication of a slowly developing enhancement or decrement in the blockade produced by halothane. Thus, the blocking effect of halothane exhibits no unusual time-dependent features and allows simple comparison of sequential applications of different concentrations of halothane. Similar reproducibility in the ability of halothane to block LVA current was observed (data not shown).

Concentration dependence of blockade of Ca^{2+} current by halothane

The concentration dependence of the reduction of Ca^{2+} current by halothane was investigated using halothane concentrations ranging from 0.1 to 5 mM. In Figure 3, the effects of three different concentrations of halothane on both LVA (Fig. 3*A,B*) and HVA (Fig. 3*C,D*) current in a single cell are illustrated. Representative examples of control currents and currents in the presence of the three concentrations of halothane are shown in

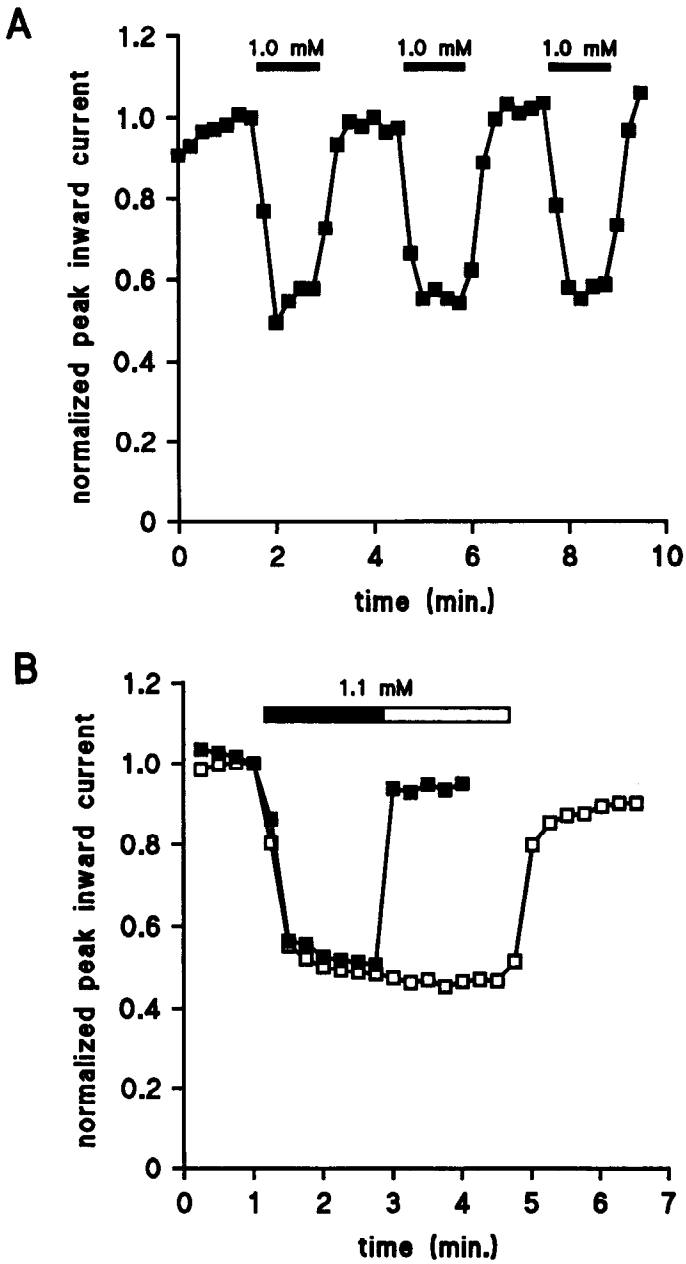

Figure 2. The blocking effect of halothane shows no time-dependent enhancement or desensitization. In *A*, HVA currents were elicited every 15 sec by the protocol shown in Figure 1. Peak inward current activated at +10 mV is plotted over time for each stimulation. For the periods indicated by the *horizontal lines*, 1.0 mM halothane was applied to the cell. The blockade produced by halothane was virtually identical for three consecutive applications. In *B*, the effect of two applications of 1.1 mM halothane applied for different durations to a different cell is shown. The HVA current was activated by stepping from a holding potential of −40 mV to 0 mV every 15 sec. Peak HVA current amplitude was normalized to the current just before halothane application. Comparison of responses in *A* and *B* indicate that there is little change in the fractional reduction of HVA Ca^{2+} current in the presence of halothane up to at least 4 min.

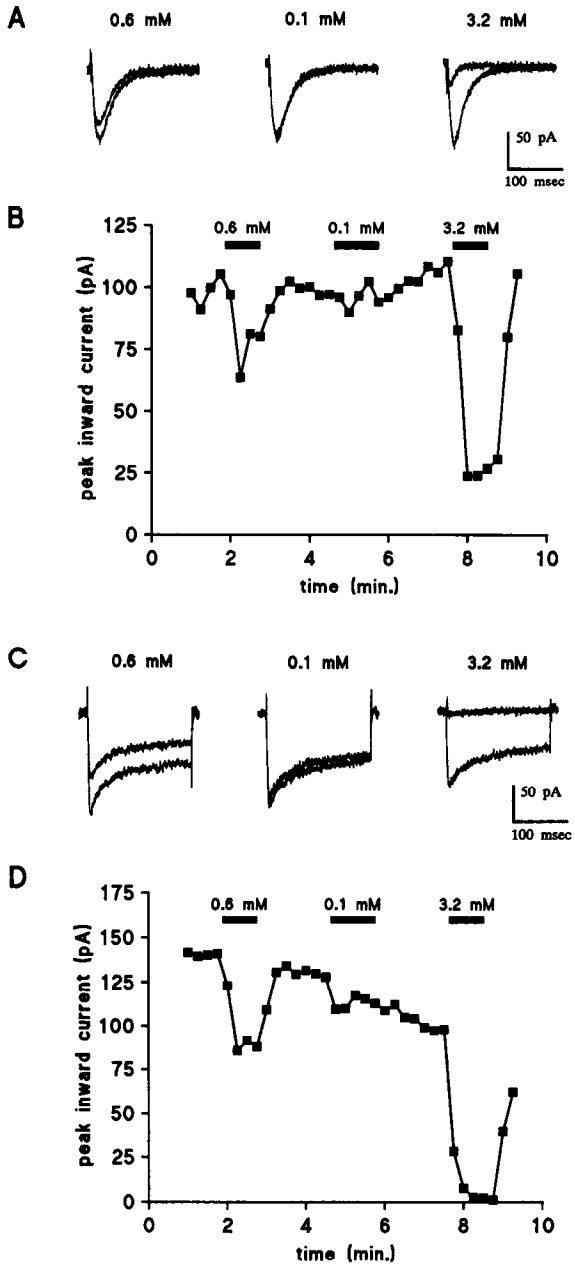

Figure 3. The blockade of Ca^{2+} current by halothane is concentration dependent. In *A*, three different concentrations of halothane were applied sequentially to a voltage-clamped GH_3 cell. From *left* to *right* across the *top*, the effects of 0.6, 0.1, and 3.2 mM halothane on LVA Ca^{2+} current are shown. In both *A* and *C*, the *horizontal bars* indicate the period of halothane application. In *B*, the peak LVA current activated at −30 mV is plotted as a function of time. In *C*, the effects of three different halothane concentrations on HVA Ca^{2+} current from the same stimulation protocols as shown in *A* are displayed. In *D*, the temporal changes in HVA current during the course of this experiment are plotted. Note that rundown of HVA current was appreciable in this cell. However, substantial recovery of HVA current was observed following virtually complete block of HVA current by 3.2 mM halothane. Traces are uncorrected for leakage and capacity currents. R_s, 14.5 MΩ.

Figure 3*A* for LVA currents and in Figure 3*C* for HVA currents. The peak inward current recorded for each command step during the course of the experiment is plotted for LVA current in Figure 3*B* and for HVA current in Figure 3*D*. Halothane is more effective in blocking HVA current than LVA current.

The concentration dependence of the halothane blocking action is summarized in Figure 4. All points were obtained using the same voltage command protocol illustrated in Figure 1. Over all experiments, HVA current is more sensitive to halothane than LVA current. The effect of halothane on peak HVA and LVA currents is compared in Figure 4*A*. The half-maximal blocking concentration is 0.85 mM for peak HVA current and 1.33 mM for peak LVA current. In the case of HVA current, complete blockade of current by halothane could be obtained. The results on LVA current suggest that at sufficiently high concentrations complete blockade may also occur. In Figure 4*B*, the concentration dependence of the blockade of peak HVA current and the HVA current remaining at the end of the command steps is compared. The half-maximal blocking concentration for the portion of HVA current remaining at the end of the command step to +10 mV is 0.5 mM.

One limitation of this analysis of the concentration dependence of halothane action is that the protocol assesses the blocking action of halothane on both LVA and HVA current at only a single command voltage and prepulse potential. Thus, if halothane were producing any substantial shift in the voltage dependence of activation of a particular current, the estimated half-maximal blocking concentration would depend on the particular protocol used to elicit the Ca^{2+} current. This issue is addressed below in the final sections of the Results.

Halothane has minimal effect on voltage-dependent Na^+ and K^+ current in GH_3 cells

In addition to Ca^{2+} current, GH_3 cells exhibit a number of voltage-dependent membrane currents that may also influence the secretory response to TRH or KCl application (Dubinsky and Oxford, 1984; Matteson and Armstrong, 1984). To determine whether the effects of halothane were selective for Ca^{2+} current, the effects of halothane on voltage-dependent K^+ and Na^+ current of GH_3 cells were also examined.

Voltage-dependent K^+ current was recorded following removal of extracellular Ca^{2+} in order to minimize the contribution of Ca^{2+}-dependent K^+ current. Under such conditions, two types of K^+ current can be observed in GH_3 cells: first, a voltage-dependent inactivating current sensitive to 4-aminopyridine (4-AP; Dubinsky and Oxford, 1984; Oxford and Wagoner, 1989), and second, a noninactivating, voltage-activated current that is at least partially blocked by 5 mM TEA (Oxford and Wagoner, 1989). Some evidence supports the view that this current reflects Ca^{2+}-activated K^+ current activated by voltage in the absence of Ca^{2+} (Oxford and Wagoner, 1989). However, at present, some contribution of a delayed-rectifier type of K^+ channel cannot be excluded. Irrespective of the identity of the noninactivating component of K^+ current, examination of the effects of halothane on these currents provides a useful comparative test of the selectivity of halothane.

Voltage-dependent K^+ currents were elicited either by voltage ramps or voltage steps. The effect of halothane on K^+ current activated by a voltage ramp is illustrated in Figure 5*A*. At command potentials above +20 mV, some blockade of K^+ current was observed with 1.2 mM halothane, with near 50% blockade observed at 3.0 mM. Halothane may produce some shift in the voltage dependence of activation of K^+ current, and as a result, the concentration dependence of halothane action will depend on the command potential. This has not been examined closely. However, the essential observation is that, at concentrations of

halothane quite effective in blocking either component of Ca^{2+} current, voltage-dependent K^+ currents are largely unaffected.

To examine the relative effectiveness of halothane on different components of K^+ current, K^+ current was evoked by depolarizations from either a −80-mV or a −40-mV holding potential. From −80 mV, a pronounced slowly inactivating K^+ current was observed, while K^+ current elicited from −40 mV was entirely noninactivating (Fig. 5*B,C*). Despite the large increase in total K^+ current elicited from a −80-mV holding potential, the absolute amount of K^+ current blocked by halothane was identical in both cases (Fig. 5*B*, bottom). This result suggests that halothane is largely selective for the noninactivating portion of K^+ current and has virtually no effect on the inactivating portion of K^+ current.

The effects of halothane on voltage-dependent Na^+ current in GH_3 cells were also examined (Fig. 6). Concentrations of 1.4 mM halothane produced only slight effects on peak Na^+ current, though both the activation and the inactivation of Na^+ current were noticeably faster at this concentration (Fig. 6*A,B*). In Figure 6, *C* and *D*, 2.6 mM halothane is shown to block peak Na^+ current about 50%. For comparison to the effects of halothane on Ca^{2+} currents, the fractional block of peak Na^+ current by halothane is plotted in Figure 4*B*.

The records in Figure 6, *A* and *C*, also show that a concentration of halothane reducing Na^+ current about 50% almost completely blocks a noninactivating outward current observed at positive command potentials. This noninactivating current is likely to represent monovalent cation flow through HVA Ca^{2+} channels (Almers et al., 1984) and thus directly demonstrates the differential sensitivity of HVA Ca^{2+} channels and Na^+ channels to halothane. Figure 6*D* illustrates the effect of halothane on the current–voltage relation of peak Na^+ current and suggests that the fractional blockade of Na^+ current by halothane is relatively independent of command potential.

Halothane also has pronounced effects on the kinetic properties of the Na^+ current. In particular, as shown in Figure 6, *A, C,* and *E,* halothane results in a pronounced increase in the rate of inactivation of Na^+ current. Furthermore, 2.6 mM halothane causes approximately an 11-mV negative shift in the steady-state inactivation curve for GH_3 cell Na^+ current (Fig. 6*F*). For four cells studied with 2.6 mM halothane, half-maximal inactivation for control Na^+ currents occurred at −61.6 ± 3.1 mV, while half-maximal inactivation was observed at −72.4 ± 2.3 mV in the presence of halothane. These effects of halothane on Na^+ current in GH_3 cells are similar to results reported for Na^+ currents in other preparations (Bean et al., 1981; Haydon and Urban, 1983). However, at concentrations that reduce Ca^{2+} current at least 50%, there is very little effect of halothane on Na^+ current (Fig. 4*B*).

The above results have established that halothane selectively reduces voltage-dependent Ca^{2+} in GH_3 cells. The remaining sections of this article will now address the possible mechanisms by which reduction of Ca^{2+} current may occur.

Effects of halothane on high-threshold Ca^{2+} current

To explore the possibility that the effect of halothane on the HVA Ca^{2+} currents is voltage dependent, HVA current was studied using both voltage steps up to +60 mV and voltage ramps up to +100 mV. Representative currents activated by different command steps from a holding potential of −40 mV are shown in Figure 7*A* both in the absence and in the presence of halothane. The peak inward current as a function of command

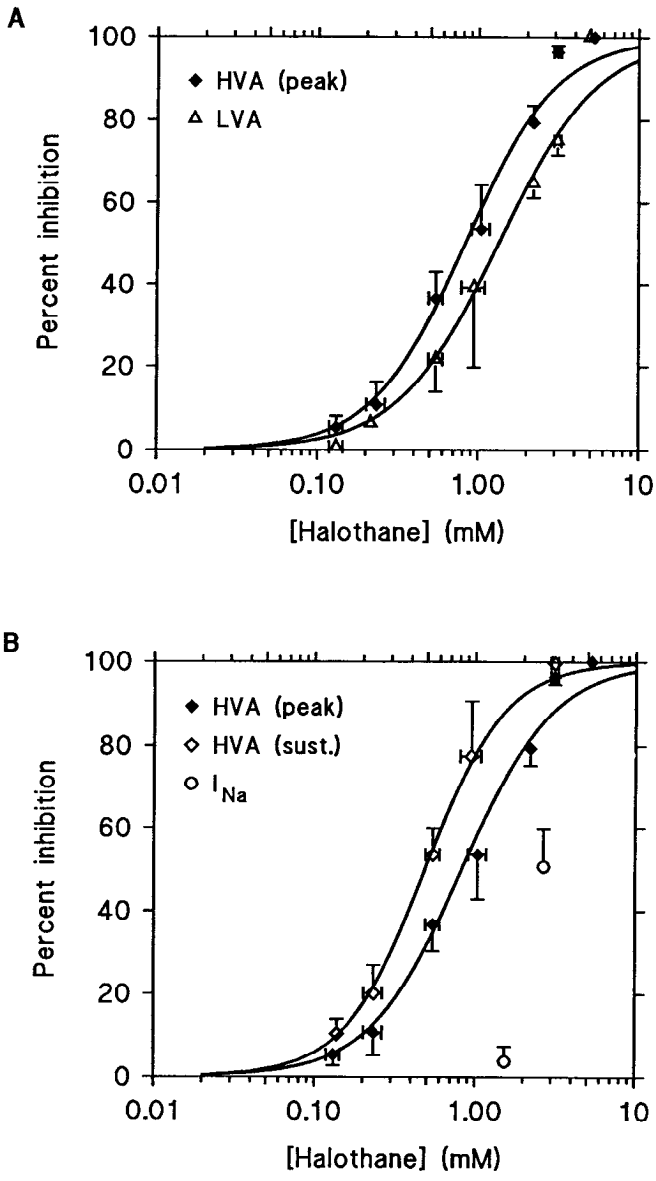

Figure 4. Concentration dependence of blockade of Ca^{2+} current by halothane. In *A*, the percent blockade of LVA (*open triangles*) and HVA (*solid diamonds*) currents are plotted versus the concentration of halothane. For display purposes, nominally identical halothane concentrations were lumped, and the mean and SD were plotted. However, for fitting purposes, all points were fit independently, and the actual measured halothane concentration was used in the fit. The percent blockade of Ca^{2+} was described by $100 - 100/(1 + ([\text{halothane}]/K_a)^n)$, where K_a represents the concentration resulting in 50% reduction of Ca^{2+} current and n represents a Hill coefficient. For blockade of LVA current, K_a = 1.3 ± 0.2 mM (±90% confidence limit on fitted value) with n = 1.4 ± 0.3. For HVA current, K_a was 0.85 ± 0.10 mM, with n = 1.5 ± 0.2. Only cells in which at least two concentrations of halothane could be examined were included in this plot, and a total of 14 cells were used. In *B*, the percent blockade of HVA current measured at the peak of the current (*solid diamonds*) and at the end of the command step (*open diamonds*) is plotted as a function of halothane concentration. The half-maximal blockade of HVA current active at the end of 190-msec voltage steps to +10 mV occurred at 0.5 ± 0.05 mM, with n = 1.75 ± 0.37. For comparison, the percent blockade of peak voltage-dependent Na^+ current (*open circles*) is plotted for two concentrations. Four cells were tested at ≈1.5 mM halothane and four cells at ≈2.7 mM.

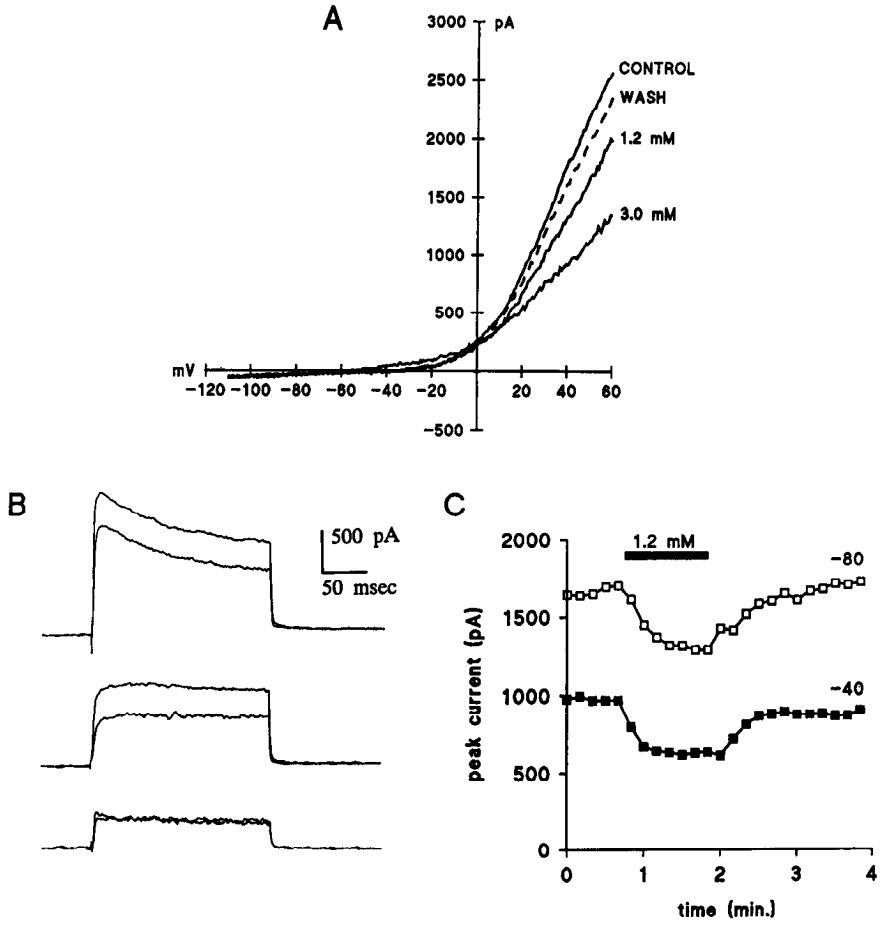

Figure 5. Effects of halothane on voltage-dependent K^+ current in GH_3 cells. In *A*, K^+ current was elicited by a 125-msec voltage ramp from −110 to +60 mV. Extracellular saline contained 0 Ca^{2+} to minimize Ca^{2+}-dependent K^+ current; 1.2 and 3 mM halothane reduce K^+ current in a concentration-dependent fashion. The apparent activation of K^+ current by 3 mM halothane at potentials negative to 0 mV was only observed in this cell. R_s, 6.4 MΩ; C_m, 17.0 pF. In *B*, the effects of 1.2 mM halothane on K^+ currents activated by command steps to +40 mV from a holding potential of −80 mV (*top*) or −40 mV (*middle*) are shown. K^+ currents activated from −80 mV exhibit a pronounced inactivating current, while currents activated from −40 mV show no inactivation. On the *bottom*, the difference between the currents activated from −40 mV and those from −80 mV either in the presence or absence of halothane are plotted. Halothane reduces the same absolute amount of current in both cases. R_s, 8.4 MΩ; C_m, 13.6 pF. In *C*, the peak K^+ current amplitudes from the experiment in *B* are plotted as a function of time for both command steps from −40 mV and from −80 mV. The amount of current removed by halothane is identical in both cases.

potential is plotted in Figure 7*B* and shows that there is no significant shift in the current–voltage relation in the presence of halothane. In particular, halothane is similarly effective in blocking Ca^{2+} current at all command potentials. However, shifts in voltage dependence of activation can be overlooked when the complete current–voltage curve is not examined (Bean, 1989b). To resolve this issue more clearly, voltage ramps were used to facilitate examination of the effect of halothane over a wider range of voltages. In the absence of tail-current measurements (Bean, 1989b), this procedure may still overlook some subtle shifts in voltage dependence of activation produced by halothane. However, as shown in Figure 7*C* (for a cell with less than 30 pA of maximal LVA current), halothane does not alter the shape of the current–voltage relationship even at voltages up to +100 mV.

HVA Ca^{2+} current in clonal pituitary cells is known to undergo inhibition by a number of mechanisms, including direct channel blockade (Cohen and McCarthy, 1987), receptor-coupled G-protein–induced modulation (Lewis et al., 1986), Ca^{2+}-induced inactivation (Kalman et al., 1988), or rundown (Armstrong and Eckert, 1987; Korn and Horn, 1989). Some experiments were done in order to provide some initial clues that might direct future investigation into the sites and mechanism of halothane action on HVA current.

To examine the possibility that the blocking action of halothane on HVA current might only develop after opening of the Ca^{2+} ion channel, the rising phase of HVA current was examined both in the absence and in the presence of halothane (Fig. 7*D*). When the current in the presence of halothane is scaled to match the peak amplitude of the control current (Fig. 7*D*), there is no detectable difference in the two currents. This is consistent with the view that there is no time-dependent aspect to the blocking action of halothane during the rising phase of the HVA current and that blockade by halothane is at equilibrium at the time of the first measurable current flow.

Halothane is known to enhance release of Ca^{2+} from the sarcoplasmic reticulum in skeletal muscle (Beeler and Gable, 1985; Mickelson et al., 1986), and it has been suggested that inhibition of Ca^{2+} current by halothane may reflect a halothane-induced elevation in intracellular Ca^{2+}, thereby mediating Ca^{2+}-dependent inactivation (Krnjević, 1974; Krnjević and Puil, 1988). Because LVA Ca^{2+} current is not thought to be subject to Ca^{2+}-dependent inactivation, it seems unlikely that elevation of $[Ca^{2+}]_i$ can account for the reduction in LVA. Several experiments were done to address the possibility that the effect of halothane on HVA current might reflect an elevation of $[Ca^{2+}]_i$ and a consequent inactivation of HVA current. First, a faster Ca^{2+} chelator, BAPTA, was used to replace EGTA in the recording pipettes. The fractional reduction of peak HVA current by 1 mM halothane in the presence of 10 mM BAPTA (50.4 ± 10.6%; $n = 3$) was indistinguishable from the reduction of HVA current by 1 mM halothane using 10 mM EGTA (53.6 ± 10.75%; $n = 11$; Fig. 4). Second, in muscle cells, halothane appears to promote release of Ca^{2+} from a caffeine-releasable pool. To test whether a similar phenomenon might account for suppression of Ca^{2+}, GH_3 cells were exposed to 10 mM caffeine prior to application of halothane. Caffeine produced no noticeable decrease in the ability of 1 mM halothane to reduce Ca^{2+} current (47.1 ± 2.1%;

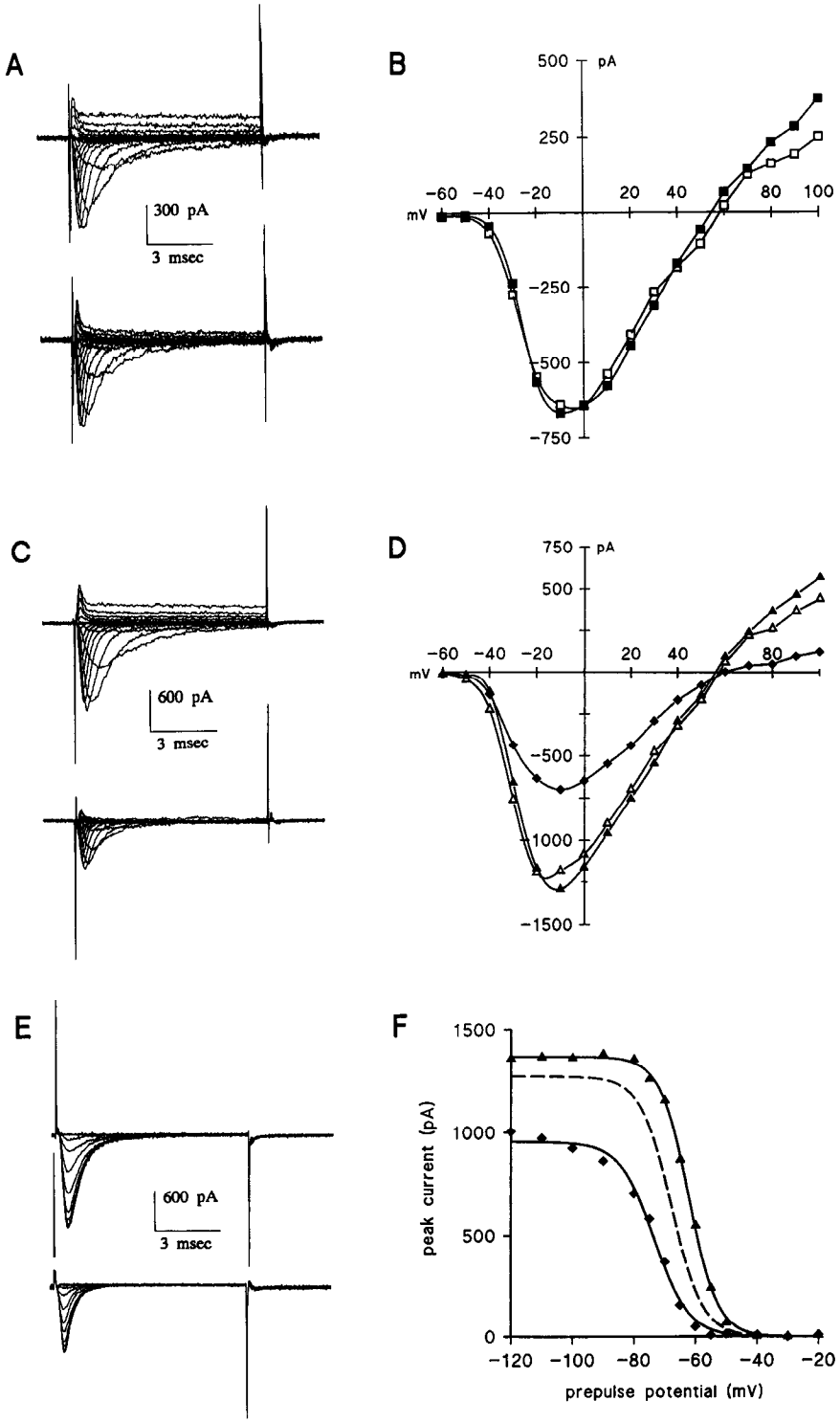

Figure 6. Effects of halothane on voltage-dependent Na^+ current in GH_3 cells. In *A*, the effect of 1.4 mM halothane on Na^+ currents activated from a holding potential of −80 mV is displayed. *Top traces,* currents in control saline; *bottom traces,* currents in 1.4 mM halothane. Halothane has little effect on peak amplitude, though alterations in current kinetics are apparent. R_s, 3.2 MΩ; C_m, 8.9 pF. In *B*, the peak amplitudes from the currents in *A* are plotted as a function of voltage to illustrate the lack of effect of halothane. *Solid squares,* control saline; *open squares,* halothane. In *C*, the effect of 2.6 mM halothane on Na^+ currents activated as in Fig. 10*A* is shown. *Top traces,* control saline; *bottom traces,* currents in 2.6 mM halothane. R_s, 3.5 MΩ; C_m, 16.3 pF. In *D*, the peak Na^+ current amplitudes are plotted from the experiment in *C*. The *diamonds* correspond to currents in halothane, while *solid* and *open triangles* correspond to currents in control saline and following recovery, respectively. In *E*, Na^+ currents were activated at −10 mV following 200 msec at potentials from −120 to −20 mV. Currents on the *top* were obtained in control saline, and currents on the *bottom,* in 2.6 mM halothane. Traces in *E* are from the same cell as in *C* and *D*. In *F*, the amplitude of currents obtained from the records in *E* are plotted as a function of inactivating voltage to yield the steady-state voltage dependence of inactivation. *Triangles* correspond to control values, *diamonds* correspond to currents in halothane, and the *broken line* indicates recovery. *Lines* represent the best-fit Boltzmann distribution: $I(V) = I_{max}/(1 + \exp[-(V - V_{50})/k])$, where I_{max} represents maximal activatable current, V_{50} represents the voltage where half the current is inactivated, and k represents the voltage dependence of the distribution. For this cell, half-maximal inactivation was −62 mV for control saline, −73 mV in halothane, and −68 mV following recovery. The slope factors describing the voltage dependence of inactivation were 4.8 mV for control saline, 5.6 mV for halothane, and 5.1 mV following recovery.

$n = 3$). However, it should be noted that both here and in the preceding article (Stern et al., 1991) we have found no evidence that caffeine activates release of Ca^{2+} from intracellular stores in GH_3 cells. This apparently contrasts with effects of caffeine in the GH_4C_1 subclone (Law et al., 1990). In any case, the result indicates that release of Ca^{2+} from at least one type of intracellular Ca^{2+} store cannot account for the reduction of Ca^{2+} current in GH_3 cells. Finally, experiments described in the preceding article (Stern et al., 1991) indicate that halothane produces no measurable increase in resting Ca^{2+} levels as measured by fura-2 fluorescence. Thus, halothane-induced reduction of HVA Ca^{2+} current in GH_3 cells is not likely to result from an elevation of $[Ca^{2+}]_i$.

Effects of halothane on voltage dependence of activation and inactivation of LVA current

In contrast to the effects of halothane on HVA current, reduction of LVA current by halothane is associated with a number of kinetic changes in the current. In particular, halothane produces changes in both activation and inactivation kinetics of LVA

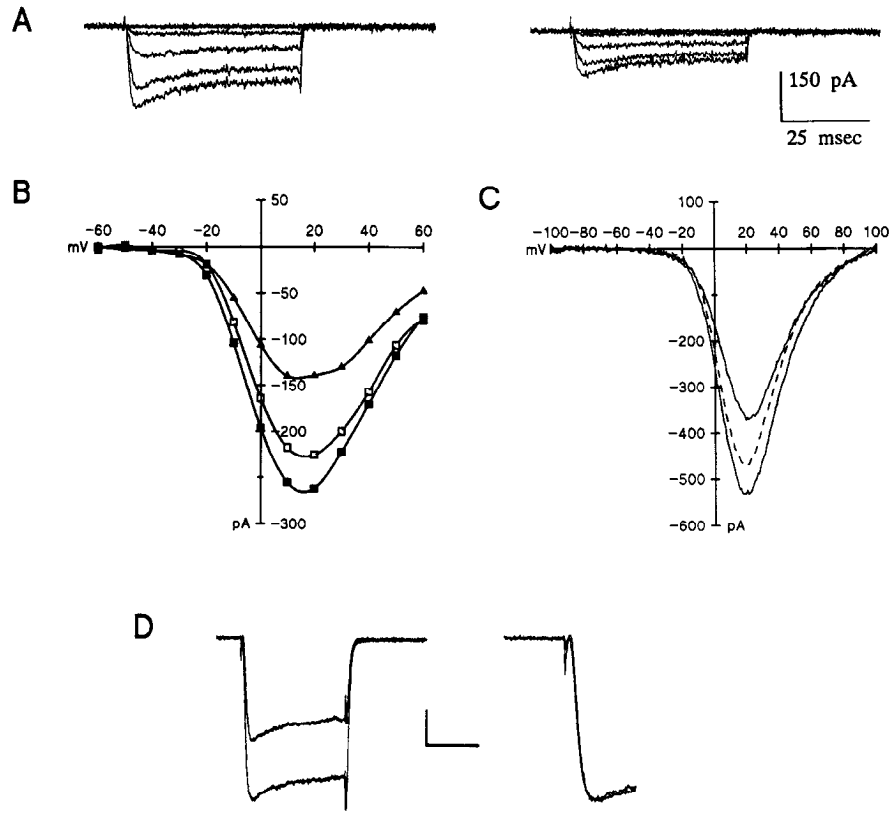

Figure 7. Effects of halothane on HVA current. In *A*, HVA currents were elicited by command steps from −30 mV through +10 mV from a holding potential of −40 mV both in the absence (*left traces*) and presence (*right traces*) of 0.9 mM halothane. R_s, 5.8 MΩ; C_m, 44.3 pF. In *B*, the peak HVA currents activated from a holding potential of −40 mV for control (*solid squares*), halothane (*triangles*), and recovery (*open squares*) salines are plotted as a function of command voltage. In *C*, to illustrate the effects of halothane at command potentials up to +100 mV, HVA current was elicited in a cell with 30 pA of LVA current by a 50-msec voltage ramp from −100 to +100 mV (4.0 mV/msec). Linear current from −60 to −100 mV was used for leakage subtraction. At least up to +80 mV, 0.9 mM halothane appears to produce a similar reduction of HVA current at all voltages. The *broken line* shows currents elicited following halothane removal. In *D*, the effect of 0.9 mM halothane on the initial rising phase of HVA current is illustrated for the same cell as in *C* (R_s, 12.2 MΩ; C_m, 23.8 pF). On the *left*, currents activated by a 100-msec step to +10 mV from a holding potential of −40 mV are shown both in the absence and presence of halothane. Calibration: vertical, 100 pA; horizontal, 25 msec. On the *right*, the currents were matched in amplitude and plotted on an expanded time base. Calibration: vertical, a.u.; horizontal, 5 msec.

current. As seen in Figures 1 and 3, the time to peak of the LVA current is shorter, and the apparent rate of inactivation somewhat faster, in the presence of halothane. These effects of halothane on LVA current kinetic properties raise the possibility that the action of halothane may involve a shift in the voltage dependence of inactivation or activation, perhaps similar to the observed effects on voltage-dependent Na^+ current.

Determination of the voltage dependence of activation of a rapidly inactivating current is complicated by a number of factors. For present purposes, there are two questions of interest. First, is the fractional blockade of LVA current produced by halothane dependent on the command potential? Second, is the alteration of LVA activation and inactivation rates sufficient to account for the reduction in peak LVA current amplitude? To assess the effect of halothane on the properties of LVA current, LVA current was examined in cells in which little or no HVA current was present. An example of the current–voltage relationship for peak LVA current in such a cell in the presence and absence of halothane is shown in Figure 8*A*. Over the range of voltages examined, there is some indication that the fractional reduction of peak LVA current produced by halothane is somewhat greater at more positive potentials. Experiments that follow provide a partial explanation for this observation.

A standard procedure for assessing the voltage dependence of activation of a current is the examination of tail-current amplitudes as a function of command voltage. As described previously (Armstrong and Matteson, 1985; Matteson and Armstrong, 1986), LVA current in GH_3 cells contributes a prominent component of slow tail current following voltage steps sufficiently short that inactivation of LVA current is minimal. At −90 mV, the inward tail current we attribute to LVA current decayed with a time constant of 2.02 ± 0.42 msec (six cells; e.g., see Fig. 9*A*). This time constant of decay of the slow tail current is similar to that previously reported for deactivation of LVA current by Matteson and Armstrong (1986) and is about an order of magnitude slower than tail-current decays associated with HVA current (Matteson and Armstrong, 1986). Experiments shown in Figure 8 also provide two pieces of evidence that the slow tails recorded here result solely from deactivation of LVA currents. First, in cells in which HVA current is largely absent (Armstrong and Eckert, 1987; Korn and Horn, 1989), the inward tail currents remain (Fig. 8*B*). As shown in Figure 8*B* in a cell in which no current was activated by steps from −40 mV to potentials from −30 to +20 mV (bottom traces), there is no slow tail current following repolarization to −40 mV. However, following command steps to various potentials from a holding potential of −90 mV, a slow tail current is evoked following repolarization to −90 mV. Second, the properties of the tail currents mirror the behavior of the LVA currents. To show this, tail currents were elicited following voltage steps of varying durations to −30 mV. The amplitudes of such tail currents as a function of command pulse duration were compared to the time course of LVA current activated at −30 mV (Fig. 8*C*). The amplitudes of the slow tail currents as a function of command pulse duration follow a time course very similar to the peak amplitude of LVA current, supporting the idea that the tail currents result from activation of LVA current. Furthermore, alteration by halothane of LVA current is mirrored by effects of halothane on tail-current amplitudes (Fig. 8*B,C*).

Having established that a component of tail current corre-

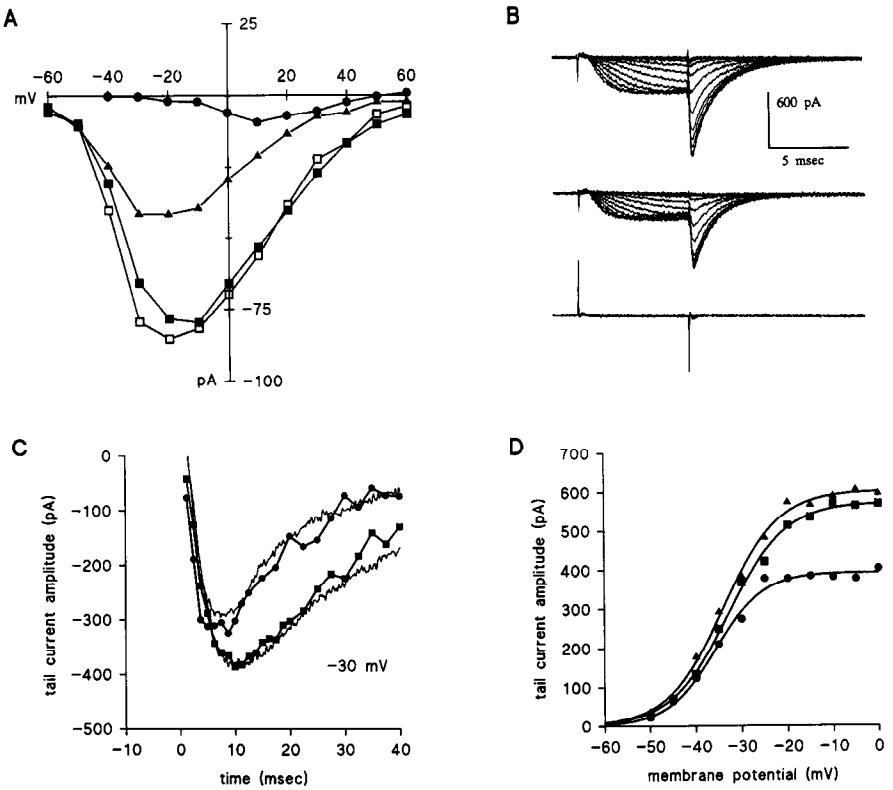

Figure 8. Effect of halothane on voltage dependence of activation of LVA current. In *A*, the amplitude of peak LVA current as a function of command potential is plotted in a cell in which there was little remaining HVA current. *Solid squares*, peak current activated from a holding potential of −90 mV in control saline; *triangles*, 2.0 mM halothane; *open squares*, wash. *Circles* plot peak inward current activated from a holding potential of −40 mV, showing that there was less than 10 pA of HVA Ca^{2+} current in this cell. In *B*, families of slow tail currents resulting from LVA current activation are shown. Inward current was elicited by a 7-msec step to command potentials between −60 and 0 mV followed by repolarization to −90 mV. A pronounced slow tail of inward current is observed at −90 mV. *Top traces*, currents in control saline; *middle traces*, 0.9 mM halothane; *bottom traces*, inward current activated by steps to −30 mV through +10 mV from a holding potential of −40 mV. No HVA current was present in this cell. Thus, the slow tail currents are specifically associated with activation of LVA current. Note the lack of effect of halothane on tail currents resulting from the smaller command steps with a more marked effect of halothane at the larger command steps. R_s, 5.2 MΩ; C_m, 12.4 pF. In *C*, families of tail currents were elicited by command steps of varying durations to −30 mV from a holding potential of −90 mV. The slow tail current was fit with a single exponential. The amplitude (*ordinate*) estimated from the exponential function both in the absence (*squares*; larger current) and presence (*circles*; smaller current) of 2.0 mM halothane is plotted as a function of the command-pulse duration (*abscissa*). The amplitude of the tail current follows a time course that mirrors the activation kinetics of LVA currents measured at −30 mV. The noisy *lines* plotted in association with the points reflect the LVA current activated at −30 mV scaled to overlap the tail-current amplitudes. The amplitude of the fitted tail currents at 250 μsec after the repolarizing voltage step was used for these plots. This may overestimate the fractional blockade produced by halothane. Halothane both shortens the time to peak LVA current and speeds the apparent time constant of inactivation. In *D*, the apparent voltage dependence of activation determined from 7-msec command steps from the cell shown in *C* is plotted. *Points* were obtained from the slow tail-current amplitude estimated from the exponential fit to the tail current. The *lines* represent the best fit of a Boltzmann distribution to each set of points. Half-maximal activation voltages for this cell were −33 mV in control saline and −36 mV in halothane. *Squares*, control saline; *circles*, halothane; *triangles*, recovery.

sponding to deactivation of LVA current can be reliably identified, the amount of LVA current activated as a function of command potential was assessed from the tail-current amplitudes. Examples of the types of traces used for assessing the effects of halothane on tail-current amplitudes are shown in Figure 8*B*. Representative tail currents in the presence and absence of halothane with the fitted exponential function overlaying the currents are displayed in Figure 9*A*. The amplitude of tail current was estimated by extrapolation of a single exponential fit to the current decay to a point 250 μsec after the initiation of the repolarization step. The effect of halothane on LVA tail-current amplitude activated by 7-msec command steps to potentials ranging from −60 to 0 mV in a cell with no HVA current is shown in Figure 8*D*. Similar to the result of Figure 8*A*, there appears to be some tendency for less blockade at the more negative activation potentials. This result implies that the estimate of half-maximal blockade of LVA current by halothane provided in Figure 4 will underestimate the blocking effect of halothane on peak LVA current at potentials positive to −30 mV and overestimate it at potentials negative to −30 mV. Although LVA currents at more negative command potentials are more resistant to blockade by halothane, the half-maximal activation voltages for control and halothane-containing salines were indistinguishable. For three cells, half-maximal activation occurred at −31.4 ± 1.1 mV for control saline and −34.1 ± 1.2 in the presence of 1 mM halothane. The slope factors indicative of the voltage dependence of the activation process were 5.9 and 4.9 for control and halothane-containing salines, respectively. Cells studied with other halothane concentrations showed qualitatively similar effects. Half-maximal activation was also estimated from the amplitudes of the maximal activatable current obtained from a Hodgkin–Huxley fit (see below)

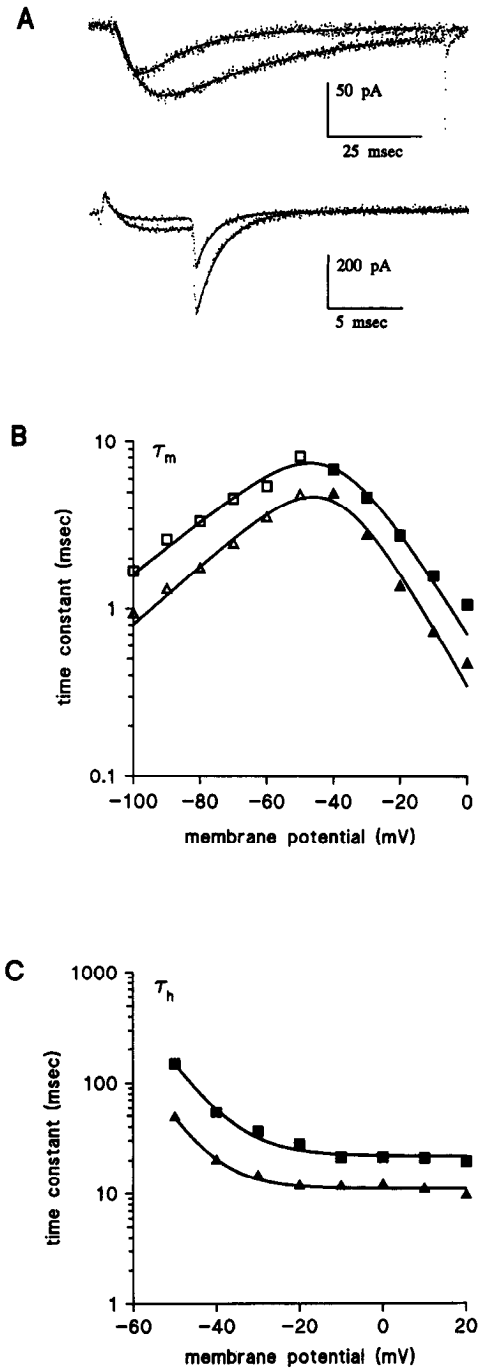

Figure 9. Alteration of kinetic properties of LVA current by halothane. In *A*, LVA currents activated by a voltage step from −90 mV to −30 mV both in the presence and absence of 2 mM halothane are displayed in the *top traces*. The best fit of a Hodgkin–Huxley activation model (Eq. 1) to the currents is overlaid over the actual current points. With $n = 2$, control values were $\tau_m = 4.8$ msec, $\tau_h = 38.5$ msec; halothane values were $\tau_m = 3.3$ msec; $\tau_h = 14.0$ msec. The *bottom traces*, from the same cell, are examples of tail currents recorded at −90 mV following the command step to −30 mV and the best single exponential fit to those currents. Control: $\tau = 1.76$ msec; 2 mM halothane: $\tau = 1.27$ msec. R_s, 4.3 MΩ; C_m, 10.6 pF. In *B*, the activation (*solid symbols*) and deactivation (*open symbols*) time constants for LVA currents obtained as in *A* either in the absence (*squares*) or in the presence (*triangles*) of 2 mM halothane are plotted as a function of membrane potential. The *lines* represent fits of Equation 2 to each set of *points* with the values as listed in the text. In *C*, the LVA current inactivation obtained from the fit of Equation 1 to the LVA current wave form is plotted as a function of command potential for currents both in the absence (*squares*) and in the presence (*triangles*) of 2 mM halothane. The *solid lines* represent the best fit of the equation $\tau(V) = 1/k(0)\cdot\exp(B\cdot V) + t_i$, where $\tau(V)$ is the observed inactivation time constant, τ_i is a voltage-independent inactivation time constant, and $k(0)$ and B represent the 0-voltage rate and voltage dependence, respectively, of the processes that contribute to the apparent voltage dependence of inactivation at voltages less than −20 mV. For this cell, the voltage-independent component of the inactivation process has a time constant of 21.8 ± 1.5 msec (90% confidence limit) in control saline and 11.1 ± 0.4 msec in 2 mM halothane.

to the LVA current. Such estimates also suggest that halothane produces little effect on the voltage dependence of activation of LVA current.

The lack of significant change in the voltage dependence of activation is further supported by an analysis of LVA current activation and deactivation rates. Figure 9 summarizes the measurements of apparent activation, deactivation, and inactivation time constants. Activation and inactivation time constants were estimated from the fit of a Hodgkin–Huxley type of model to the entire LVA current time course as follows:

$$I(t) = A\cdot(1\ \exp(-t/\tau_m))^n\cdot\exp(-t/\tau_h), \quad (1)$$

where m, h, and n have their usual meanings (Hodgkin and Huxley, 1952; Yoshii et al., 1988) and A is a scaling factor representing maximal activatable current. The onset of current activation particularly at potentials negative to −30 mV exhibits some sigmoidicity requiring that n be at least 2. However, the value of n, though affecting the exact value of t_m, is not critical to any of the conclusions reached below. The deactivation time constant was estimated as in Figure 9*A* from a single exponential fit to the tail currents following activation of LVA current. The most prominent effect of halothane is a shortening of the activation rate constant and deactivation rate constant over the entire voltage range (Fig. 9*B*). For a Hodgkin–Huxley approximation, the activation time constant or deactivation time constant as a function of membrane potential is

$$\tau_m(V) = 1/[\alpha_m(V) + \beta_m(V)], \quad (2)$$

where $\alpha_m(V)$ and $\beta_m(V)$ represent apparent activation and deactivation rates, respectively. When Equation 2 is fit to the points in Figure 9*B*, the following values for the 0-voltage kinetic rates (units of $msec^{-1}$) and the voltage dependencies (units of mV^{-1}) were obtained:

$$\alpha(V) = 1.117\cdot\exp(0.067\cdot V),$$

and

$$\beta(V) = 0.014\cdot\exp(-0.038\cdot V).$$

In 2 mM halothane, the corresponding expressions were

$$\alpha(V) = 4.354\cdot\exp(0.094\cdot V),$$

and

$$\beta(V) = 0.022\cdot\exp(-0.040\cdot V).$$

Qualitatively similar results were obtained in four cells with halothane concentrations of either 1 or 2 mM. The essential feature of the action of halothane is that there is little change in the voltage dependence for either apparent rate, though there is an increase in each rate. The magnitude of the increase appears to depend on the concentration of halothane (not shown).

For control currents, the voltage at which the apparent activation time constant equals the deactivation time constant is about −45 mV. At this voltage, the channel opening rate equals the channel closing rate, and as such, this voltage provides another estimate of the half-maximal LVA current activation under steady-state conditions. It is notable that halothane does not change this voltage at which the activation rate is identical to the deactivation rate (Fig. 9*B*). This probably provides the best indication that halothane has minimal effect on the voltage dependence of activation of the LVA current.

The properties of the apparent inactivation rate of LVA current are more complex. Figure 9*A* provides an example of the effect of halothane on the inactivation of LVA current. Over the range of −60 to −20 mV, the apparent inactivation time constant decreases with depolarization. Presumably at the more negative potentials, the apparent inactivation rate is complicated by the slow rate of activation of the current. Above −20 mV, the inactivation rate is fairly voltage independent. Halothane produces an increase in the apparent inactivation rate at all voltages (Fig. 9*C*). For three cells tested with halothane, the voltage-independent inactivation rate was 49.7 ± 10/sec in control saline and 75.2 ± 12.1/sec in 2 mM halothane. Lower concentrations of halothane produced smaller changes in this rate.

To assess whether the changes in activation, deactivation, and inactivation rates could account for the reduction in peak LVA current amplitude, two separate types of models were considered. This included the Hodgkin–Huxley expression shown above (Eq. 1) and a five-state model proposed to describe T-current behavior in 3T3 fibroblasts (both schemes 3a and 3b from Chen and Hess, 1990). In the latter case, predicted currents were generated using a Runge–Kutta procedure to solve the appropriate set of differential equations. For all cases, the alteration in kinetic behavior was insufficient to explain the reduction in peak LVA current amplitude by halothane. In particular, the observed effect of halothane on activation and deactivation kinetics is expected to result in a shift in the time to peak LVA current (e.g., as seen in Figs. 8, 9) with little change in amplitude. The effect on inactivation kinetics would result in some reduction in peak current amplitude, which would be somewhat more pronounced at more positive activation voltages (e.g., as in Fig. 8*D*), but the magnitude of the observed changes in inactivation rates is insufficient with either type of model to account for the magnitude of the reduction in peak current. Two possible explanations are the following: First, some of the reduction of peak current by halothane could be explained by schemes in which halothane increases the number of channels that enter inactivated states without ever opening. Second, halothane might reduce the single-channel conductance of the underlying currents. However, whatever the explanation of the reduction in peak current, to account for the smaller inhibition at more negative command potentials (Fig. 8*D*) this process would need to be rather voltage dependent. For this reason, at present we prefer the explanation that halothane affects rates of inactivation from closed states of the LVA channel.

To test the possibility that the voltage-dependence of inactivation might contribute to the reduction of LVA current by halothane, the effects of halothane on the steady-state inactivation properties of LVA current are illustrated in Figure 10. LVA current was elicited by command steps to −30 mV following periods of 500 msec at prepulse potentials ranging from −120 to −40 mV. Typical families of currents elicited by such a protocol are shown in Figure 10*A* for control saline, saline containing 1.2 mM halothane, and recovery. As observed above, the time to peak and rate of inactivation of LVA current are faster in the presence of halothane. The LVA current activated as a function of prepulse potential is plotted in Figure 10*B*. The LVA current activated as a function of prepulse normalized to the maximal activatable current is plotted as a function of prepulse potential in Figure 10*C* in order to emphasize the relative lack of effect of halothane. In each case, the points were fit by a single Boltzmann distribution. For three cells tested with 1 mM halothane, half-maximal inactivation was observed at −52.7 ± 0.9 mV in control saline and −55.4 ± 1.9 mV in halothane. The slope factors in each case were 5.9 and 6.0 mV, respectively. Thus, halothane produces little effect on the voltage dependence of inactivation of LVA current.

Discussion

The major finding of this article is that halothane reduces two components of voltage-dependent Ca^{2+} current in clonal GH_3 pituitary cells. HVA Ca^{2+} current is more sensitive to halothane than LVA Ca^{2+} current, but both currents are substantially more sensitive to halothane than either voltage-dependent Na^+ current, a 4-AP–sensitive, inactivating voltage-dependent K^+ current, or a noninactivating component of voltage-dependent K^+ current. Coupled with results from the preceding article (Stern et al., 1991), the halothane-induced inhibition of TRH- and KCl-induced prolactin secretion in GH_3 cells appears to result from the reduction of Ca^{2+} current by halothane. Furthermore, these results support the view that, at clinically relevant concentrations, volatile anesthetics do not produce some nonspecific alteration in a large number of membrane-associated processes. In particular, within the clinically relevant range of concentrations, we found that, of the processes we have examined, only Ca^{2+} current is sensitive to halothane.

Concentration dependence of halothane action on Ca^{2+} current

The concentration of halothane that produces 50% blockade of peak HVA current is about 0.8 mM; the concentration producing 50% blockade of LVA current, when measured at −30 mV command potential, is about 1.3 mM. Several factors influence the usefulness of these numbers for comparison to other effects of halothane in other preparations. Because little voltage dependence was observed in the inhibition of either current by halothane, these half-maximal blocking estimates should be largely independent of stimulation protocol. However, a noticeable component of inactivating HVA current was observed in many cells, and the percent blockade of current at the end of command steps was clearly greater than at the peak of the HVA current. In fact, 50% blockade of HVA current at the end of depolarizing commands to +20 mV occurred at about 0.5 mM halothane. Without a better understanding of the origin of the apparent inactivation of HVA current, it is difficult to assess the significance of the interaction of halothane with the inactivation. In most cases, the absolute amount of HVA current exhibiting inactivation appears identical in the presence or absence of halothane. This would seem to be most easy to reconcile with a situation in which there is both a noninactivating HVA current sensitive to halothane and an inactivating portion of HVA current relatively resistant to halothane (though blocked at sufficiently high concentrations; see Fig. 3*A*, 3.2 mM halothane). However, the results cannot exclude the possibility that halothane, acting on a single population of HVA channels, shifts

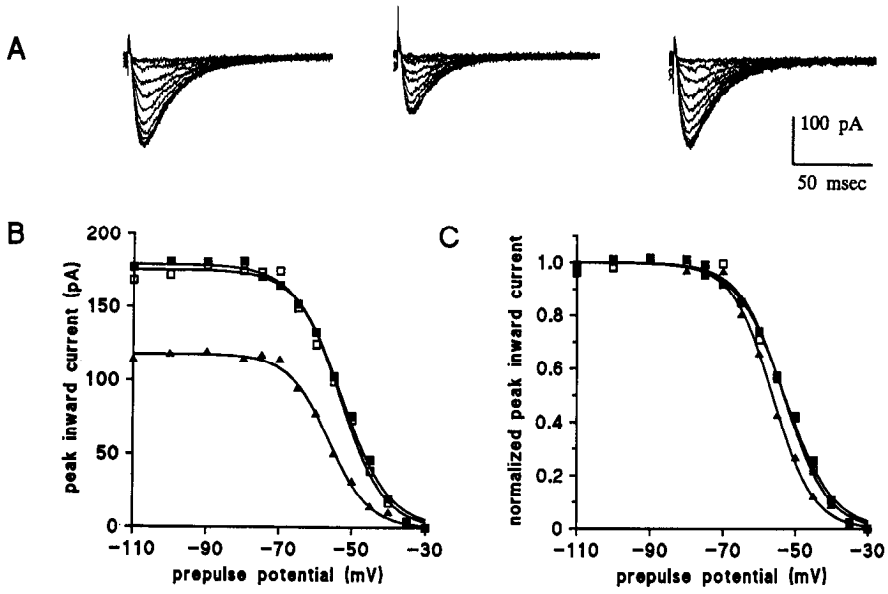

Figure 10. Halothane has little effect on the voltage dependence of inactivation of LVA current. In *A*, LVA currents were activated at −20 mV following periods of 500 msec at voltages from −110 to −30 mV. The *left* and *right* sets of traces show control and recovery currents, respectively, while currents in the presence of 1.2 mM halothane are shown in the *middle*. R_s, 12.5 MΩ; C_m, 10.8 pF. In *B*, the peak amplitudes from the traces in *A* are plotted as a function of voltage. *Solid squares* are control values, *open squares* are recovery values, and *triangles* are values in 1.2 mM halothane. The fit of a Boltzmann distribution to the points is plotted over each set of points (*lines*). For this cell, half-maximal inactivation occurred at −53 mV in control saline and −56 mV in halothane. In *C*, the points in *B* are plotted after normalization to the peak current amplitude in each case to better illustrate the minimal effect of halothane. *Symbols* are as in *B*.

the relative distribution among inactivated, open, and closed states.

The sensitivity of LVA current in GH_3 cells is markedly less than the reported sensitivity (50% block at 0.1 mM halothane) of an LVA Ca^{2+} current in rat DRG cells (Takenoshita and Steinbach, 1990). In addition to the apparent difference in sensitivity to halothane between GH_3 and dorsal root ganglion cell LVA Ca^{2+} current, the activation kinetics of the two currents are quite different. The observed differences may reflect the existence of distinct types of LVA currents in these two cell types.

Mechanism of action of halothane

Reduction of HVA Ca^{2+} current can occur by any of a number of mechanisms, including receptor-coupled G-protein–induced inhibition (Lewis et al., 1986), direct pharmacological blockade (Cohen and McCarthy, 1987), Ca^{2+}-mediated inactivation (Kalman et al., 1988), or rundown possibly involving dephosphorylation (Armstrong and Eckert, 1987). Our results, though not in any way conclusive, support the view that halothane acts directly on the Ca^{2+} channel.

The possibility that Ca^{2+}-mediated inactivation of HVA current (Krnjević, 1974; Krnjević and Puil, 1988) plays a role in the effects of halothane is unlikely for three reasons: First, halothane produced no increase in resting levels of Ca^{2+} in GH_3 cells (Stern et al., 1991). Second, the effect of halothane was similar whether 10 mM BAPTA or 10 mM EGTA was used in the intracellular pipette. It is unlikely that the release of Ca^{2+} from intracellular stores could appreciably elevate submembrane Ca^{2+} under such conditions. Third, a caffeine-releasable pool of intracellular Ca^{2+}, a potential target of halothane action (Beeler and Gable, 1985; Mickelson et al., 1986), does not appear to be present in GH_3 cells. The present results also provide some information concerning the idea that halothane reduces HVA current either by mimicking the action of a G-protein or by activating a somatostatin-sensitive G-protein that inhibits the Ca^{2+} current (Lewis et al., 1986). A characteristic of G-protein–mediated inhibition of HVA current in some cells is slowing of activation and relief of blockade during depolarizing pulses at very positive potentials (Luini et al., 1986; Bean, 1989b; Dolphin and Scott, 1989; Ikeda and Schofield, 1989). This was not observed in the case of halothane. In addition, in preliminary experiments the fractional reduction of HVA current produced by halothane and time course of onset and recovery of halothane blockade was identical following inclusion of the non-hydrolyzable guanosine triphospate analog, GTP-γ-S, in the recording micropipettes. Thus, these arguments suggest that involvement of G-proteins in the mechanism of halothane-induced reduction of HVA Ca^{2+} current is unlikely.

The final point concerning the mechanism of blockade of HVA current is that blockade appears to exhibit no significant time dependence during the initial 10–20 msec of activation of HVA current. This supports the view that, whatever the mechanism of blockade, blockade is fully developed at the time of the first sampling point on the first activation of current in the presence of halothane. Unfortunately, it was not possible to distinguish whether blockade requires opening of the channel or whether blockade develops in the absence of channel opening.

In contrast to the effect of halothane on HVA current, halothane produced marked alterations in the kinetic properties of LVA current. Such an alteration of kinetic behavior could result from both direct and indirect actions of halothane on the LVA channels, and the present results do not allow us to discriminate between these possibilities. However, in terms of understanding the mechanism of reduction of LVA current, it is important to know whether the alteration in kinetic properties can account entirely for the blockade of LVA current. Although the present results were not intended as a detailed analysis of GH_3 LVA-channel kinetic properties, an attempt was made to correlate the halothane-induced alterations in kinetic behavior with the effects of halothane on steady-state inactivation, activation, and fractional blockade. Our results indicate that the halothane-induced increases in activation and inactivation rates were not sufficient to account for all the reduction of peak LVA current. This discrepancy suggests that halothane may also reduce the maximal number of LVA channels that can be opened during a command step or reduce the current flow through the channels. The effects of halothane on LVA kinetics are similar in some ways to the effect of halothane on Na^+ current in which sub-

stantial alteration of Na^+ current kinetics is observed at concentrations of halothane that produce negligible change in the peak Na^+ current amplitude.

Specificity in halothane action

One significant feature of this work is that the effect of halothane on a number of different cellular processes and potential sites of action was evaluated. Although halothane inhibits several different membrane currents, effects of halothane on Ca^{2+} currents occurred at substantially lower concentrations. In addition, halothane was without noticeable effect on a number of other phenomena that involve membrane-associated biochemical steps. Halothane did not produce an elevation of intracellular Ca^{2+} in resting cells, nor did it inhibit the ability of TRH to produce an inositol triphosphate–mediated elevation of $[Ca^{2+}]_i$ (Stern et al., 1991). Similarly, halothane was without effect on the ability of thyrotropin-releasing hormone (TRH) to stimulate phosphoinositide hydrolysis (Stern et al., 1991). Thus, our results support the view that, at clinically relevant concentrations, only a limited number of membrane-associated processes are altered by halothane. In particular, we found that, of the processes we have examined, only Ca^{2+} current is sensitive to halothane and only the reduction in Ca^{2+} current can account for the halothane-induced reduction of KCl- and TRH-induced secretion.

Physiological significance of Ca^{2+} current inhibition by halothane

Clearly, alteration of Ca^{2+} channel function can have critical consequences for a number of cellular processes and, in particular, for synaptic transmission. It remains unclear which HVA Ca^{2+} channels may be involved in synaptic transmission (Bean, 1989a), and evidence in support of both L- and N-types of channels has been presented (Rane et al., 1987; Hirning et al., 1988). If an L-type HVA Ca^{2+} channel analogous to those in GH_3 cells was involved in synaptic transmission, halothane would be expected to produce inhibition of synaptic transmission. However, it should be kept in mind that the functional categories of LVA and HVA Ca^{2+} current may represent families of channels with distinct pharmacological sensitivities such that effects of halothane on Ca^{2+} channels in GH_3 cells may not relate to effects on particular neuronal preparations. Thus, the potential consequences of L-current inhibition by halothane must await better definition of the physiological role of different categories of HVA current in different neurons.

Our results show that the effects of halothane on HVA Ca^{2+} current in GH_3 cells occur within a clinically appropriate range (0.2–0.9 mM). However, it is unclear to what extent the relatively modest reductions in Ca^{2+} current amplitude at concentrations less than 0.5 mM halothane would be functionally meaningful. Two issues address this question: First, in the case of synaptic transmission, the large cooperativity in the Ca^{2+} dependence of transmitter release (Dodge and Rahamimoff, 1967; Dingledine and Somjen, 1981; Llinas et al., 1981) would imply that small changes in Ca^{2+} influx might have large effects on amount of transmitter released. Thus, small reductions may be sufficient to produce substantial depression of Ca^{2+}-dependent processes. Second, it is interesting to consider that the magnitude of inhibition of Ca^{2+} current produced by endogenous modulatory actions typically involves less than 50% blockade of Ca^{2+} current even at maximal concentrations of inhibitor (Lewis et al., 1986; Bean, 1989b; Dolphin and Scott, 1989; Ikeda and Schofield, 1989). Thus, significant functional alterations may be expected to occur in response to relatively modest reductions in Ca^{2+} current.

Because of the large number of effects of volatile anesthetics that have been described, there is some opinion that the anesthetic effect may not result from action on a single functional target. Our results support the view that, though halothane may affect multiple components of membrane current in GH_3 cells, only Ca^{2+} currents are sensitive to halothane within the clinical concentration range. At least in GH_3 cells, halothane exhibits clear specificity in its action. However, it is clear that other effects of halothane do occur in appropriate concentration ranges (Nicoll and Madison, 1982; Franks and Lieb, 1988). One view supported by the present work is that, though there may be multiple clinically important molecular targets of general anesthetic action, the number of these targets may be more limited than often imagined.

References

Almers W, McCleskey EW, Palade PT (1984) A non-selective cation conductance in frog muscle membrane blocked by micromolar external calcium ions. J Physiol (Lond) 353:565–583.

Armstrong CM, Matteson DR (1985) Two distinct populations of calcium channels in a clonal line of pituitary cell. Science 227:65–67.

Armstrong D, Eckert R (1987) Voltage-activated calcium channels that must be phosphorylated to respond to membrane depolarization. Proc Natl Acad Sci USA 84:2518–2522.

Bean BP (1989a) Classes of calcium channels in vertebrate cells. Annu Rev Physiol 51:367–384.

Bean BP (1989b) Neurotransmitter inhibition of neuronal calcium currents by changes in channel voltage dependence. Nature 340:153–156.

Bean BP, Shrager P, Goldstein DA (1981) Modification of sodium and potassium channel gating kinetics by ether and halothane. J Gen Physiol 77:233–253.

Beeler T, Gable K (1985) Effect of halothane on Ca^{2+}-induced Ca^{2+} release from sarcoplasmic reticulum vesicles isolated from rat skeletal muscle. Biochim Biophys Acta 821:142–152.

Bossu JL, Feltz A, Thomann JM (1985) Depolarization elicits two distinct calcium currents in vertebrate sensory neurones. Pfluegers Arch 403:360–368.

Carbone E, Lux HD (1984) A low voltage–activated, fully inactivating Ca channel in vertebrate sensory neurones. Nature 310:501–502.

Carbone E, Lux HD (1987) Kinetics and selectivity of a low-voltage-activated calcium current in chick and rat sensory neurones. J Physiol (Lond) 386:547–570.

Chen C, Hess P (1990) Mechanism of gating of T-type calcium channels. J Gen Physiol 96:603–630.

Cherkin A, Catchpool JF (1964) Temperature dependence of anesthesia in goldfish. Science 144:1460–1462.

Cohen CJ, McCarthy RT (1987) Nimodipine block of calcium channels in rat anterior pituitary cells. J Physiol (Lond) 387:195–225.

Dingledine R, Somjen G (1981) Calcium dependence of synaptic transmission in the hippocampal slice. Brain Res 207:218–222.

Dodge RA, Rahamimoff R (1967) Co-operative action of calcium ions in transmitter release at the neuromuscular junction. J Physiol (Lond) 193:419–432.

Dolphin AC, Scott RH (1989) Interaction between calcium channel ligands and guanine nucleotides in cultured rat sensory and sympathetic neurones. J Physiol (Lond) 413:271–288.

Dubinsky JM, Oxford GS (1984) Ionic currents in two strains of rat anterior pituitary tumor cells. J Gen Physiol 83:309–339.

Eskinder H, Supan FD, Rusch NJ, Kampine JP, Bosnjak ZJ (1990) Effects of halothane (HAL) on Ca^{++} channel currents in canine cardiac Purkinje cells. Biophys J 57:518a.

Evers AS, Elliott WJ, Lefkowith JB, Needleman P (1986) Manipulation of rat brain fatty acid composition alters volatile anesthetic potency. J Clin Invest 77:1028–1033.

Fox AP, Nowycky MC, Tsien RW (1987) Kinetic and pharmacological properties distinguishing three types of calcium currents in chick sensory neurones. J Physiol (Lond) 394:149–172.

Franks NP, Lieb WR (1988) Volatile general anaesthetics activate a novel neuronal K^+ current. Nature 333:662–664.

Hamill OP, Marty E, Neher E, Sakmann B, Sigworth FJ (1981) Improved patch-clamp techniques for high-resolution current recording from cells and cell-free membrane patches. Pfluegers Arch 381:85–100.

Haydon DA, Urban BW (1983) The effects of some inhalation anaesthetics on the sodium current of the squid giant axon. J Physiol (Lond) 341:429–439.

Herrington J, Lingle CJ (1990) Halothane reduces calcium currents in clonal (GH_3) pituitary cells. New York Academy of Sciences Conference on Molecular and Cellular Mechanisms of Alcohol and Anesthetics, abstract W-6.

Hirning LD, Fox AP, McCleskey EW, Olivera BM, Thayer SA, Miller RJ, Tsien RW (1988) Dominant role of N-type Ca^{2+} channels in evoked release of norepinephrine from sympathetic neurons. Science 239:57–61.

Hodgkin AL, Huxley AF (1952) A quantitative description of membrane current and its application to conduction and excitation in nerve. J Physiol (Lond) 117:500–544.

Holz GG IV, Dunlap K, Kream RM (1988) Characterization of the electrically evoked release of substance P from dorsal root ganglion neurons: methods and dihydropyridine sensitivity. J Neurosci 8:463–471.

Ikeda SR, Schofield GG (1989) Somatostatin blocks a calcium current in rat sympathetic ganglion neurones. J Physiol (Lond) 409:221–240.

Ikemoto Y, Yatani A, Imoto Y, Arimura H (1986) Reduction in the myocardial sodium current by halothane and thiamylal. Jpn J Physiol 36:107–121.

Kalman D, O'Lague PH, Erxleben C, Armstrong DL (1988) Calcium-dependent inactivation of the dihydropyridine-sensitive calcium channels in GH_3 cells. J Gen Physiol 92:531–548.

Korn SJ, Horn R (1989) Influence of sodium–calcium exchange on calcium current rundown and the duration of calcium-dependent chloride currents in pituitary cells, studied with whole cell and perforated patch recordings. J Gen Physiol 94:789–812.

Kostyuk PG, Shuba YM, Savchenko AN (1988) Three types of calcium channels in the membrane of mouse sensory neurons. Pfluegers Arch 411:661–669.

Krnjević K (1974) Central actions of general anaesthetics. In: Molecular mechanisms in general anasethesia (Halsey MJ, Millar R, Sutton JA, eds), pp 65–89. New York: Churchill Livingstone.

Krnjević K, Puil E (1988) Halothane suppresses slow inward currents in hippocampal slices. Can J Physiol Pharmacol 66:1570–1575.

Kullmann DM, Martin RL, Redman SJ (1989) Reduction by general anaesthetics of group Ia excitatory postsynaptic potentials and currents in the cat spinal cord. J Physiol (Lond) 412:277–296.

Larrabee MG, Posternak JM (1954) Selective action of anesthetics on synapses and axons in mammalian sympathetic ganglia. J Neurophysiol 15:91–114.

Law GJ, Pachter JA, Thastrup O, Hanley MR, Dannies PS (1990) Thapsigargin, but not caffeine, blocks the ability of thyrotropin-releasing hormone to release Ca^{2+} from an intracellular store in GH_4C_1 cells. Biochem J 267:359–364.

Lewis DL, Weight FF, Luini A (1986) A guanine-nucleotide binding protein mediates the inhibition of voltage-dependent calcium current by somatostatin in a pituitary cell line. Proc Natl Acad Sci USA 83: 9035–9039.

Llinas R (1988) The intrinsic electrophysiological properties of mammalian neurons: insights into central nervous system function. Science 242:1654–1664.

Llinas R, Yarom Y (1981) Electrophysiology of mammalian inferior olivary neurones *in vitro*. Different types of voltage-dependent ionic conductances. J Physiol (Lond) 315:549–567.

Llinas R, Steinberg IZ, Walton K (1981) Relationship between presynaptic calcium current and postsynaptic potential in squid giant synapse. Biophys J 33:323–352.

Luini A, Lewis D, Guild S, Schofield G, Weight F (1986) Somatostatin, an inhibitor of ACTH secretion, decreases cytoplasmic free calcium and voltage-dependent calcium current in a pituitary cell line. J Neurosci 6:3128–3132.

Matteson DR, Armstrong CM (1984) Na and Ca channels in a transformed line of anterior pituitary cells. J Gen Physiol 83:371–394.

Matteson DR, Armstrong CM (1986) Properties of two types of calcium channels in clonal pituitary cells. J Gen Physiol 87:161–182.

Mickelson JR, Ross JA, Reed BK, Louis CF (1986) Enhanced Ca^{2+}-induced calcium release by isolated sarcoplasmic reticulum vesicles from malignant hyperthermia susceptible pig muscle. Biochim Biophys Acta 862:318–328.

Miu P, Puil E (1989) Isoflurane-induced impairment of synaptic transmission in hippocampal neurons. Exp Brain Res 75:354–360.

Nicoll RA, Madison DV (1982) General anesthetics hyperpolarize neurons in the vertebrate central nervous system. Science 217:1055–1057.

Oxford GS, Wagoner PK (1989) The inactivating K^+ current in GH_3 pituitary cells and its modification by chemical reagents. J Physiol (Lond) 410:587–612.

Pearce RA, Stringer JL, Lothman EW (1989) Effect of volatile anesthetics on synaptic transmission in the rat hippocampus. Anesthesiology 71:591–598.

Rane SG, Holz GG IV, Dunlap K (1987) Dihydropyridine inhibition of neuronal calcium current and substance P release. Pfluegers Arch 409:361–366.

Regan MJ, Eger EI (1967) II. Effect of hypothermia in dogs on anesthetizing and apneic doses of inhalation agents. Anesthesiology 28: 689–700.

Richards CD (1983) Actions of general anaesthetics on synaptic transmission in the CNS. Br J Anaesth 55:201–207.

Richards CD, Smaje JC (1976) Anaesthetics depress the sensitivity of cortical neurones to L-glutamate. Br J Pharmacol 58:347–357.

Ruppersberg JP, Rudel R (1988) Differential effects of halothane on adult and juvenile sodium channels in human muscle. Pfluegers Arch 412:17–21.

Stern RC, Weiss CI, Steinbach JH, Evers AS (1989) Isoflurane uptake and elimination are delayed by absorption of anesthetic by the scimed membrane oxygenator. Anesth Analg 69:657–662.

Stern RC, Herrington J, Lingle CJ, Evers AS (1991) The action of halothane on stimulus–secretion coupling in clonal (GH_3) pituitary cells. J Neurosci 11:2217–2225.

Suzuki S, Rogawski MA (1989) T-type calcium channels mediate the transition between tonic and phasic firing in thalamic neurons. Proc Natl Acad Sci USA 86:7228–7232.

Takenoshita M, Steinbach JH (1990) Halothane blocks low-voltage-activated calcium currents in rat sensory neurons. Soc Neurosci Abstr 16:511.

Takenoshita M, Takahashi T (1987) Mechanisms of halothane action on synaptic transmission in motoneurons of the newborn rat spinal cord *in vitro*. Brain Res 402:303–310.

Terrar DA, Victory JGG (1988) Effects of halothane on membrane currents associated with contraction in single myocytes isolated from guinea-pig ventricle. Br J Pharmacol 94:500–508.

Yoshii M, Tsunoo A, Narahashi T (1988) Gating and permeation properties of two types of calcium channels in neuroblastoma cells. Biophys J 54:885–895.